

DISCRETE CONSTANT ENVELOPE TRANSCEIVER DESIGN FOR MULTIUSER MASSIVE MIMO DOWNLINK

Mingjie Shao[†], Qiang Li[‡] and Wing-Kin Ma[†]

[†] Department of Electronic Engineering, The Chinese University of Hong Kong, Hong Kong SAR, China

[‡] School of Info. & Commun. Engineering, University of Electronic Science and Technology of China

ABSTRACT

This paper considers multiuser massive MIMO downlink transmission, where the base station (BS) employs a massive number of transmit antennas, each equipped with a low-resolution phase shifter, to simultaneously shape desired symbols at user side, after passing through the channels and receive beamforming. This channel-aided shaping technique, known as symbol-level nonlinear precoding, has recently gained considerable attention owing to its high power efficiency and low implementation cost. However, the design of the transmit signal itself is challenging because the restriction of the transmit signals to a discrete constant envelope (DCE) set leads to a discrete optimization problem. In this paper, we adopt a minimum symbol-error probability design criterion for joint optimization of the transmit DCE signal at the BS and the receive beamformers at the users. An alternating minimization method is built for the problem. The design of the transmit DCE signal leverages on a negative square penalty (NSP) method developed in our recent work. The design of receive beamformers can be decoupled among users and updated by non-convex gradient projection independently. Our simulation results show that the bit-error rate performance markedly improves as the number of receive antennas increases.

Index Terms— multiuser massive MIMO, discrete constant envelope, minimum symbol-error probability

1. INTRODUCTION

The trend of using massive MIMO in wireless communication systems has recently triggered great interest in constant envelope (CE) precoding methods. While massive MIMO is promising in providing high spectral efficiency and many other benefits, power consumption and hardware cost are becoming a bottleneck for the development of massive MIMO. CE precoding, in which cheap phase shifters are deployed at the base station (BS), provides a solution to overcome this issue. By using the phase shifters, the demand for large linear-amplification dynamic ranges of the power amplifiers can be relaxed significantly. In practice, phase shifters only have finite discrete phase combinations rather than continuous phase states, which raises an issue in CE precoding designs. This paper will focus on the discrete CE (DCE) transceiver design.

Most existing works assume continuous phase shifters. Some early works [1, 2] conducted a full study of CE precoding for the single-user MISO case. Shortly afterward, some CE precoding designs for the multiuser MISO case emerged using different approaches [3–7]. A constellation independent approach, which minimizes multiuser interference power in the least squares sense, was adopted in [3–5]. A constructive interference approach, which exploits the PSK constellation structure, was proposed in [6]. Recently, these formulations were extended to tackle the more challenging

DCE precoder designs [8, 9]. As a remark, we should mention that the emerging one-bit precoding problem can be regarded as a special case of the DCE precoding problem. Interested readers are referred to [10–12] for details. As our latest endeavor, a systematic approach for minimization of symbol-error probabilities was proposed in [13] for one-bit, continuous CE and DCE precoding. The research advances in this topic, as it stands, are with the multiuser MISO case. On the other hand, it is well known that multiuser MIMO, in which users can perform receive beamforming, has great potential in system performance enhancement.

In this paper, we take a step ahead into the realm of multiuser MIMO DCE precoding by extending our very recent developed technique in [13]. Or, this paper can be seen as a conference version of [13], with new elements (multiuser MIMO) not seen in [13]. We propose to jointly optimize the transmit DCE precoder and the receive beamformers to minimize the symbol-error probabilities (SEPs). By applying alternating minimization, we update the DCE precoder and receive beamformers in an alternating fashion. The update for the DCE precoder is done by applying the techniques proposed in [13], while the update for receive beamformers can be decoupled among users, and a non-convex gradient projection method is employed to optimize the receive beamformers. Simulation results indicate that the BER performance can be significantly enhanced when the number of receive antennas increases.

2. PROBLEM FORMULATION

Consider a multiuser MIMO downlink transmission scenario, where a BS with N transmit antennas sends K separate data streams to K users, one for each user. For simplicity, we assume that each user has M receive antennas. The scenario is depicted in Fig. 1. Let $\mathbf{x}_t \in \mathbb{C}^N$ be the transmit signal at time t . The receive signals at the users are given by

$$\mathbf{y}_{i,t} = \mathbf{H}_i \mathbf{x}_t + \mathbf{n}_{i,t}, \quad i = 1, \dots, K, \quad t = 1, \dots, T, \quad (1)$$

where $\mathbf{y}_{i,t} \in \mathbb{C}^M$ is the receive signal of user i at time slot t ; T is the transmission block length; $\mathbf{H}_i \in \mathbb{C}^{M \times N}$ is the downlink channel associated with user i , which is assumed to be unchanged during the transmission block (i.e., the so-called block fading assumption); $\mathbf{n}_{i,t}$ is additive noise, and it is assumed that $\mathbf{n}_{i,t} \sim \mathcal{CN}(\mathbf{0}, \sigma^2 \mathbf{I})$. At the user side, each user performs receive beamforming

$$\mathbf{z}_{i,t} = \mathbf{v}_i^H \mathbf{y}_{i,t} = \mathbf{v}_i^H \mathbf{H}_i \mathbf{x}_t + \mathbf{v}_i^H \mathbf{n}_{i,t}, \quad (2)$$

where $\mathbf{v}_i \in \mathbb{C}^M$ is the receive beamformer for user i .

Herein, the BS employs phase shifters with finite phase combinations to generate the transmit signal \mathbf{x}_t , that is, each element of \mathbf{x}_t is drawn from a discrete set with constant envelope. In particular,

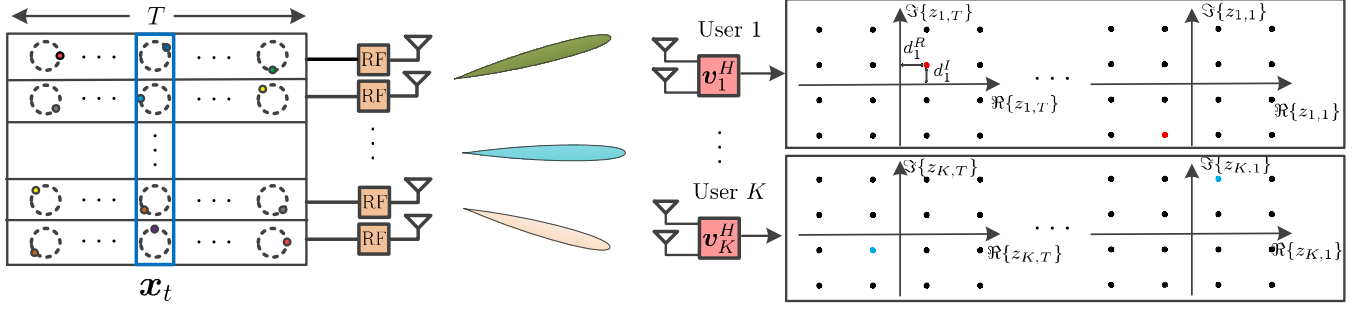


Fig. 1: The scenario.

we write $\mathbf{x}_t = \sqrt{\frac{P}{N}} \mathbf{u}_t$, $\mathbf{u}_t \in \mathcal{U}^N$, where P is the total transmission power at the BS, and

$$\mathcal{U} \triangleq \{u = e^{j(\frac{2\pi}{L}l + \frac{\pi}{L})} \mid l = 0, \dots, L-1\} \quad (3)$$

with L being some positive even integer. Fig. 2 illustrates an example of the set \mathcal{U} . Note that the one-bit precoding problem is a special case of (3) with $L = 4$, as illustrated in Fig. 1(a).

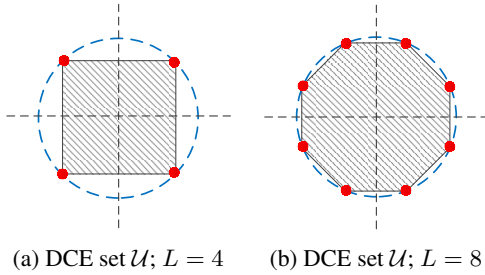


Fig. 2: Illustration of DCE set; the red points are the elements in \mathcal{U}

We aim to jointly design the precoder $\{\mathbf{u}_t\}_t$ and the receive beamformers $\{\mathbf{v}_i\}_i$ such that all the users can successfully recover their desired symbols $\{s_{i,t}\}_t$ from $\{z_{i,t}\}_t$ with minimal chances of error. In this work, we focus on the QAM constellation, i.e.,

$$s_{i,t} \in \mathcal{S} \triangleq \{s_R + js_I \mid s_R, s_I \in \{\pm 1, \pm 3, \dots, \pm(2B-1)\}\}, \forall i, t \quad (4)$$

for some positive integer B , and we adopt the SEP as our design metric. To this end, each user detects the symbols by

$$\hat{s}_{i,t} = \text{dec}(\Re\{z_{i,t}\}/d_i^R) + j \cdot \text{dec}(\Im\{z_{i,t}\}/d_i^I), \quad (5)$$

where $\text{dec}(\cdot)$ is the decision function for $\{\pm 1, \pm 3, \dots, \pm(2B-1)\}$; d_i^R and d_i^I represent the inter-point spacings of the received symbol in the in-phase and quadrature direction for user i , resp. (see Fig. 1). Note that the decoding performance also depends on d_i^R and d_i^I , and thus they need to be jointly optimized with $\{\mathbf{u}_t\}_t$ and $\{\mathbf{v}_i\}_i$. Readers are referred to [11, 13] for more explanations on the inter-point spacings.

With (1)-(5), the conditional SEP is defined as

$$\text{SEP}_{i,t} = \Pr(\hat{s}_{i,t} \neq s_{i,t} \mid s_{i,t}). \quad (6)$$

We will simply call (6) SEP in the sequel. Now, our problem of interest is to minimize the worst SEP over all the users and over the

whole transmission block, which reads

$$\begin{aligned} \min_{\mathbf{U}, \mathbf{d}, \mathbf{V}} \max_{i=1, \dots, K} \text{SEP}_{i,t} \\ \text{s.t. } \mathbf{U} \in \mathcal{U}^{N \times T}, \mathbf{d} \geq 0, \|\mathbf{v}_i\|^2 = 1, i = 1, \dots, K, \end{aligned} \quad (7)$$

where $\mathbf{U} = [\mathbf{u}_1, \dots, \mathbf{u}_T]$; $\mathbf{V} = [\mathbf{v}_1, \dots, \mathbf{v}_T]$; $\mathbf{d} = [(d^R)^T, (d^I)^T]^T$, $\mathbf{d}^R = [d_1^R, \dots, d_K^R]^T$, $\mathbf{d}^I = [d_1^I, \dots, d_K^I]^T$. Note that, without loss of generality, each receive beamformer \mathbf{v}_i is assumed to have unit norm, $\|\mathbf{v}_i\|^2 = 1$, $\forall i$.

2.1. SEP Approximation

The exact SEP expression in (6) was shown in [13]. It does not admit an easy-to-optimize form, and thus we turn to tractable approximation. By extending our exact SEP expression for the multiuser MISO case in [13], it can be shown the SEP in (6) is bounded by

$$\max\{\text{SEP}_{i,t}^R, \text{SEP}_{i,t}^I\} \leq \text{SEP}_{i,t} \leq 2 \max\{\text{SEP}_{i,t}^R, \text{SEP}_{i,t}^I\}, \quad (8)$$

where

$$\text{SEP}_{i,t}^R \leq 2 \max \left\{ Q \left(\frac{\sqrt{2}b_{i,t}^R}{\sigma \|\mathbf{v}_i\|} \right), Q \left(\frac{\sqrt{2}c_{i,t}^R}{\sigma \|\mathbf{v}_i\|} \right) \right\}, \quad (9a)$$

$$b_{i,t}^R = d_i^R - \left(\sqrt{\frac{P}{N}} \Re\{\mathbf{v}_i^H \mathbf{H}_i \mathbf{u}_t\} - d_i^R \Re\{s_{i,t}\} \right), \quad (9b)$$

$$c_{i,t}^R = d_i^R + \left(\sqrt{\frac{P}{N}} \Re\{\mathbf{v}_i^H \mathbf{H}_i \mathbf{u}_t\} - d_i^R \Re\{s_{i,t}\} \right), \quad (9c)$$

$\text{SEP}_{i,t}^I$, $b_{i,t}^I$ and $c_{i,t}^I$ are defined in the same way as $\text{SEP}_{i,t}^R$, $b_{i,t}^R$ and $c_{i,t}^R$ by replacing “ \Re ” and “ R ” in (9) with “ \Im ” and “ I ”, resp., and, $Q(x) = \int_x^\infty \frac{1}{\sqrt{2\pi}} e^{-z^2/2} dz$. In the following, we focus on minimizing the SEP upper bound in (9a).

2.2. Problem Reformulation

Applying (8)-(9) into (7), and using the monotonicity of $Q(\cdot)$, we can consider

$$\begin{aligned} \min_{\mathbf{U}, \mathbf{d}, \mathbf{V}} \max_{i,t} \left\{ -b_{i,t}^R, -b_{i,t}^I, -c_{i,t}^R, -c_{i,t}^I \right\} \\ \text{s.t. } \mathbf{U} \in \mathcal{U}^{N \times T}, \mathbf{d} \geq 0, \|\mathbf{v}_i\|^2 = 1, i = 1, \dots, K. \end{aligned} \quad (10)$$

as a replacement of problem (7). It is more convenient to convert problem (10) to a real-valued problem. It can be shown that

$$\Re\{\mathbf{v}_i^H \mathbf{H}_i \mathbf{u}_t\} = \tilde{\mathbf{v}}_i^T \tilde{\mathbf{H}}_i \tilde{\mathbf{u}}_t, \quad \Im\{\mathbf{v}_i^H \mathbf{H}_i \mathbf{u}_t\} = \tilde{\mathbf{v}}_i^T \tilde{\tilde{\mathbf{H}}}_i \tilde{\mathbf{u}}_t, \quad (11)$$

where

$$\begin{aligned} \bar{\mathbf{v}}_i &= [\Re(\mathbf{v}_i)^T \Im(\mathbf{v}_i)^T]^T, \bar{\mathbf{u}}_t = [\Re(\mathbf{u}_t)^T \Im(\mathbf{u}_t)^T]^T, \\ \bar{\mathbf{H}}_i &= \begin{bmatrix} \Re(\mathbf{H}_i) & -\Im(\mathbf{H}_i) \\ \Im(\mathbf{H}_i) & \Re(\mathbf{H}_i) \end{bmatrix}, \tilde{\mathbf{H}}_i = \begin{bmatrix} \Im(\mathbf{H}_i) & \Re(\mathbf{H}_i) \\ -\Re(\mathbf{H}_i) & \Im(\mathbf{H}_i) \end{bmatrix}. \end{aligned}$$

Then, the real-valued equivalent form of (10) is given by

$$\begin{aligned} \min_{\bar{\mathbf{U}}, \mathbf{d}, \bar{\mathbf{V}}} f_{\text{orig}}(\bar{\mathbf{U}}, \mathbf{d}, \bar{\mathbf{V}}) &\triangleq \max_{i,t} \left\{ -b_{i,t}^R, -b_{i,t}^I, -c_{i,t}^R, -c_{i,t}^I \right\} \\ \text{s.t. } \text{cpl}(\bar{\mathbf{U}}) &\in \mathcal{U}^{N \times T}, \mathbf{d} \geq 0, \|\bar{\mathbf{v}}_i\|^2 = 1, i = 1, \dots, K, \end{aligned} \quad (12)$$

where $\bar{\mathbf{U}} = [\bar{\mathbf{u}}_1, \dots, \bar{\mathbf{u}}_T]$; $\bar{\mathbf{V}} = [\bar{\mathbf{v}}_1, \dots, \bar{\mathbf{v}}_K]$; $\tilde{\mathbf{X}} = \text{cpl}(\mathbf{X})$ is an operator that maps a real-valued matrix $\mathbf{X} \in \mathbb{R}^{2n \times m}$ into a complex-valued matrix $\tilde{\mathbf{X}} \in \mathbb{C}^{n \times m}$ through the relation $\mathbf{X} = [\Re(\tilde{\mathbf{X}})^T, \Im(\tilde{\mathbf{X}})^T]^T$.

3. PROPOSED SOLUTION FOR PROBLEM (11)

Problem (12) is non-smooth and non-convex. To tackle it, we leverage on our recently proposed negative penalty (NSP) method [13]. The NSP method reformulates problem (12) as

$$\begin{aligned} \min_{\bar{\mathbf{U}}, \mathbf{d}, \bar{\mathbf{V}}} f_{\text{orig}}(\bar{\mathbf{U}}, \mathbf{d}, \bar{\mathbf{V}}) - \lambda \sum_{t=1}^T \|\bar{\mathbf{u}}_t\|^2 \\ \text{s.t. } \text{cpl}(\bar{\mathbf{U}}) \in \bar{\mathcal{U}}^{N \times T}, \mathbf{d} \geq 0, \|\bar{\mathbf{v}}_i\|^2 = 1, i = 1, \dots, K, \end{aligned} \quad (13)$$

where $\bar{\mathcal{U}} \triangleq \text{conv } \mathcal{U}$ is the convex hull of \mathcal{U} , as illustrated as the shaded area in Fig. 2; $\lambda > 0$ is a penalty parameter. Intuitively, the NSP reformulation relaxes the DCE set \mathcal{U} as its convex hull $\bar{\mathcal{U}}$, and at the same time it adds an NSP term to the objective to force the solution to a vertex of $\bar{\mathcal{U}}$, i.e., a point in \mathcal{U} . It is shown in [13, Theorem 1] that for a sufficiently large λ , problems (12) and (13) are equivalent. The important advantage of NSP is that the NSP reformulation (13) now has convex constraints with respect to $\bar{\mathbf{U}}$, rather than discrete DCE constraints as in the original problem.

We apply alternating minimization to problem (13), with the transmit signals and the receive beamformers optimized in an alternating fashion. The algorithm is summarized in Algorithm 1, where GEMM and GP stand for the GEMM algorithm for updating $(\bar{\mathbf{U}}, \mathbf{d})$ and gradient projection (GP) algorithm for updating $\bar{\mathbf{V}}$, resp., which will be introduced in the next subsections. Note that the penalty parameter λ is increased every J iteration (cf. line 5). We found that, empirically, this strategy is effective in speeding up the convergence.

Algorithm 1 Alternating Minimization for Problem (13)

- 1: Given a starting point $\bar{\mathbf{U}}^0, \mathbf{d}^0, \bar{\mathbf{V}}^0$, an initial $\lambda > 0$, a threshold $\lambda_{\text{upp}} > 0$, an integer J , a constant $c > 1$.
 - 2: **for** $k = 0, 1, 2, \dots$ **do**
 - 3: Update $(\bar{\mathbf{U}}^{k+1}, \mathbf{d}^{k+1}) = \text{GEMM}(\bar{\mathbf{U}}^k, \mathbf{d}^k, \bar{\mathbf{V}}^k)$;
 - 4: Update $\bar{\mathbf{v}}_i^{k+1} = \text{GP}(\bar{\mathbf{U}}^{k+1}, \mathbf{d}^{k+1}, \bar{\mathbf{v}}_i^k), i = 1, \dots, K$;
 - 5: Update $\lambda = \lambda \times c$ every J iterations.
 - 6: **end for** when $\lambda > \lambda_{\text{upp}}$.
-

Next, we will specify the GEMM and GP algorithms.

3.1. The Update for $(\bar{\mathbf{U}}, \mathbf{d})$

When the receive beamforming matrix $\bar{\mathbf{V}}$ in problem (13) is fixed, problem (13) reduces to a virtual MISO precoding problem and can

be handled by the GEMM algorithm proposed in [13]. In view of space limit, we will only give a high-level description of GEMM.

First, we apply smooth approximation, namely log-sum-exp approximation, to the objective of (13), which leads to

$$\min_{\bar{\mathbf{U}}, \mathbf{d}} f(\bar{\mathbf{U}}, \mathbf{d}, \bar{\mathbf{V}}) - \lambda \sum_{t=1}^T \|\bar{\mathbf{u}}_t\|^2 \quad (14a)$$

$$\text{s.t. } \text{cpl}(\bar{\mathbf{U}}) \in \bar{\mathcal{U}}^{N \times T}, \mathbf{d} \geq 0, \quad (14b)$$

where $f(\bar{\mathbf{U}}, \mathbf{d}, \bar{\mathbf{V}}) \triangleq \mu \log \left(\sum_{i=1}^K \sum_{t=1}^T f_{i,t}(\bar{\mathbf{u}}_t, \mathbf{d}, \bar{\mathbf{v}}_i) \right)$ with $f_{i,t}(\bar{\mathbf{u}}_t, \mathbf{d}, \bar{\mathbf{v}}_i) = e^{-b_{i,t}^R/\mu} + e^{-b_{i,t}^I/\mu} + e^{-c_{i,t}^R/\mu} + e^{-c_{i,t}^I/\mu}$; $\mu > 0$ is a smoothing parameter, and $f(\bar{\mathbf{U}}, \mathbf{d}, \bar{\mathbf{V}}) \rightarrow f_{\text{orig}}(\bar{\mathbf{U}}, \mathbf{d}, \bar{\mathbf{V}})$ as $\mu \rightarrow 0$.

Second, we apply majorization-minimization (MM) to handle the smoothed problem (14). Notice that $f(\bar{\mathbf{U}}, \mathbf{d}, \bar{\mathbf{V}})$ is convex w.r.t. $(\bar{\mathbf{U}}, \mathbf{d})$ for fixed $\bar{\mathbf{V}}$. Hence, (14a) is in the form of difference-of-convex (DC) function, which can be handled by MM. Specifically, we repeatedly solve the following majorization problem of (14):

$$\min_{\bar{\mathbf{U}}, \mathbf{d}} f(\bar{\mathbf{U}}, \mathbf{d}, \bar{\mathbf{V}}) - 2\lambda \sum_{t=1}^T (\bar{\mathbf{u}}_t^j)^T (\bar{\mathbf{u}}_t - \bar{\mathbf{u}}_t^j) \quad (15)$$

$$\text{s.t. } \text{cpl}(\bar{\mathbf{U}}) \in \bar{\mathcal{U}}^{N \times T}, \mathbf{d} \geq 0,$$

where $\bar{\mathbf{u}}_t^j$ represents the last MM iteration result and j is the MM iteration index. For such a smooth convex problem, one can apply the gradient projection method to solve it. Its iterative update reads

$$\begin{aligned} \bar{\mathbf{U}}^{i+1} &= \Pi_{\bar{\mathcal{U}}^{N \times T}}(\bar{\mathbf{U}}^i - \beta_i \nabla_{\bar{\mathbf{U}}} f(\bar{\mathbf{U}}^i, \mathbf{d}^i)); \\ \bar{\mathbf{d}}^{i+1} &= \Pi_{\mathbb{R}_+^{2K}}(\bar{\mathbf{d}}^i - \beta_i \nabla_{\bar{\mathbf{d}}} f(\bar{\mathbf{U}}^i, \mathbf{d}^i)); \end{aligned} \quad (16)$$

where β_i is the step size at iteration i ; $\Pi_{\mathcal{X}}(\mathbf{x}) = \arg \min_{\mathbf{y} \in \mathcal{X}} \|\mathbf{x} - \mathbf{y}\|^2$ denotes the projection of \mathbf{x} onto \mathcal{X} . The projection $\Pi_{\mathbb{R}_+^{2K}}$ can simply be done by thresholding. For $\Pi_{\bar{\mathcal{U}}^{N \times T}}$, it suffices to consider $\Pi_{\bar{\mathcal{U}}}$. Curiously, it is shown that $\Pi_{\bar{\mathcal{U}}}$ has a simple closed-form solution [13]; specifically, we have

$$\Pi_{\bar{\mathcal{U}}}(u) = e^{j \frac{2\pi n}{L}} \left([\Re(\tilde{u})]_0^{\cos(\pi/L)} + j [\Im(\tilde{u})]_{-\sin(\pi/L)}^{\sin(\pi/L)} \right), \quad (17)$$

where

$$n = \left\lfloor \frac{\angle u + \pi/L}{2\pi/L} \right\rfloor, \quad \tilde{u} = ue^{-j \frac{2\pi n}{L}}.$$

It should be noted that the MM described above is not exactly the method we eventually use to handle (15). As an improvement, we do not solve the MM subproblem (15) exactly; instead we apply one-step extrapolated gradient descent to update the solution of (15). With such inexact MM update, we found that the algorithm empirically runs much faster than exact MM, and moreover, it also possesses the same convergence guarantees as exact MM. This algorithm is called GEMM, and readers are referred to [13] for full details.

3.2. The Update for $\bar{\mathbf{V}}$

Given $\bar{\mathbf{U}}$ and \mathbf{d} , the update of $\bar{\mathbf{V}}$ requires solving

$$\begin{aligned} \min_{\bar{\mathbf{V}}} \max_{i,t} \left\{ -b_{i,t}^R, -b_{i,t}^I, -c_{i,t}^R, -c_{i,t}^I \right\} \\ \text{s.t. } \|\bar{\mathbf{v}}_i\|^2 = 1, i = 1, \dots, K. \end{aligned} \quad (18)$$

By noticing that the $\bar{\mathbf{v}}_i$'s are independent both in the objective function and constraints, problem (18) can be decoupled among users. Specifically, the optimization of each $\bar{\mathbf{v}}_i$ is done by solving

$$\begin{aligned} \min_{\bar{\mathbf{v}}_i} g_{\text{orig}}(\bar{\mathbf{v}}_i) &\triangleq \max_t \left\{ -b_{i,t}^R, -b_{i,t}^I, -c_{i,t}^R, -c_{i,t}^I \right\} \\ \text{s.t. } &\|\bar{\mathbf{v}}_i\|^2 = 1. \end{aligned} \quad (19)$$

Similarly, we apply log-sum-exp smooth approximation to recast the problem (19) as

$$\min_{\bar{\mathbf{v}}_i} g(\bar{\mathbf{v}}_i) \quad \text{s.t. } \|\bar{\mathbf{v}}_i\|^2 = 1, \quad (20)$$

where $g(\bar{\mathbf{v}}_i) = \eta \log \left(\sum_{t=1}^T g_{i,t}(\bar{\mathbf{u}}_t, \mathbf{d}, \bar{\mathbf{v}}_i) \right)$ for $\eta > 0$, and $g_{i,t}(\bar{\mathbf{u}}_t, \mathbf{d}, \bar{\mathbf{v}}_i) = e^{-b_{i,t}^R/\eta} + e^{-b_{i,t}^I/\eta} + e^{-c_{i,t}^R/\eta} + e^{-c_{i,t}^I/\eta}$. We use the GP method to handle the subproblem (20):

$$\bar{\mathbf{v}}_i^{j+1} = \Pi_{\mathcal{V}}(\bar{\mathbf{v}}_i^j - \gamma_j \nabla_{\bar{\mathbf{v}}_i} g(\bar{\mathbf{v}}_i^j)),$$

where j is the iteration index; γ_j is the step size and is determined by backtracking line search [14]; $\mathcal{V} \triangleq \{\mathbf{v}_i \mid \|\mathbf{v}_i\|^2 = 1\}$, and

$$\Pi_{\mathcal{V}}(\mathbf{x}) = \begin{cases} \text{any } \tilde{\mathbf{x}} \text{ with } \|\tilde{\mathbf{x}}\|^2 = 1, & \text{if } \mathbf{x} = \mathbf{0}, \\ \mathbf{x}/\|\mathbf{x}\|, & \text{otherwise.} \end{cases}$$

It is known that the above GP method guarantees convergence to a critical point of problem (20) [15].

4. SIMULATION RESULTS

In this section, we evaluate the performance of the proposed algorithm by Monte-Carlo simulations. We measure the bit error rate (BER) averaged over 5,000 channel trials. The transmission block length is $T = 10$. The elements of channel \mathbf{H}_i are i.i.d. generated from $\mathcal{CN}(0, 1)$ in each trial. The total transmission power at BS is $P = 1$. The BS is equipped with $N = 128$ antennas.

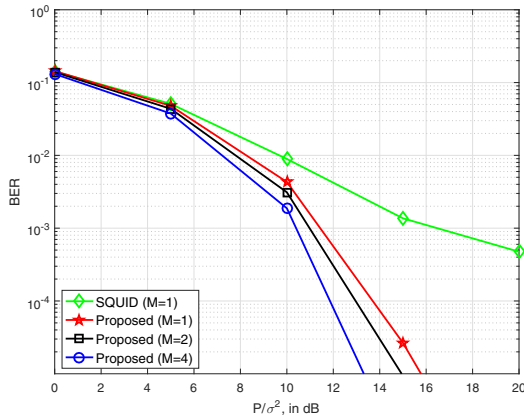


Fig. 3: BER performance of DCE precoding for different numbers of receive antennas. 16-QAM, $L = 4$.

For Algorithm 1, the smoothing parameters are $\mu = 0.05$ and $\eta = 0.01$. The sub-algorithm GEMM is stopped when the difference of successive iterates satisfies $\|\bar{\mathbf{U}}^{j+1} - \bar{\mathbf{U}}^j\|_F^2 + \|\mathbf{d}^{j+1} - \mathbf{d}^j\|^2 \leq 10^{-4}$ or when the maximum iteration 200 is reached; GP is stopped when $\|\bar{\mathbf{v}}_i^{j+1} - \bar{\mathbf{v}}_i^j\|^2 \leq 10^{-4}$ or when the maximum iteration 200 is

reached. The penalty parameter λ is initialized as 0.01, and we set $\lambda_{\text{upp}} = 100$, $J = 5$ and $c = 5$.

Figs. 3 and 4 show the BER performance for the one-bit case, i.e., $L = 4$. There are $K = 16$ users. Fig. 3 considers the 16-QAM constellation, while Fig. 4 the 64-QAM constellation. The benchmarked algorithm ‘‘SQUID’’ proposed in [10] is a popular algorithm for one-bit precoding for the multiuser MISO case. We see that the BER performance improves as the number of receive antennas increases. In particular, in Fig. 4, adding one more antennas ($M = 2$) at user sides leads to an SNR gain over 5dB compared with the MISO case.

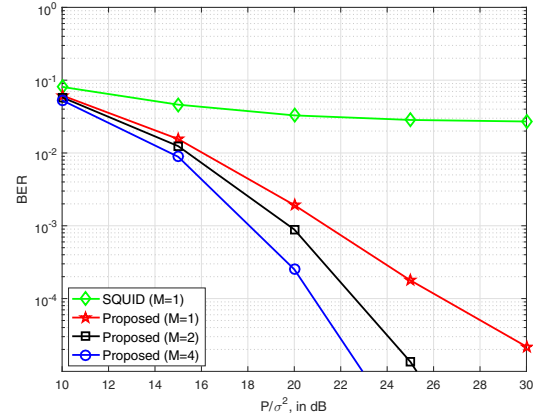


Fig. 4: BER performance of DCE precoding for different numbers of receive antennas. 64-QAM, $L = 4$.

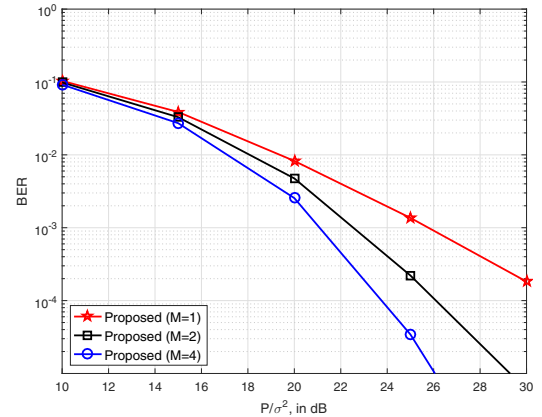


Fig. 5: BER performance of DCE precoding for different numbers of receive antennas. 64-QAM, $L = 8$.

Fig. 5 shows the BER performance of the DCE case with $L = 8$. There are $K = 32$ users. 64-QAM is used for transmission. Again, we see that adding receive antennas improves the BER performance.

5. CONCLUSION

In this paper, we have considered a joint design of transmit DCE precoding and receive beamforming for the multiuser massive MIMO scenario. Simulation results suggest that employing multiple antennas at the user side is beneficial in enhancing the BER performance.

6. REFERENCES

- [1] S. K. Mohammed and E. G. Larsson, "Single-user beamforming in large-scale MISO systems with per-antenna constant-envelope constraints: The doughnut channel," *IEEE Trans. Wireless Commun.*, vol. 11, no. 11, pp. 3992–4005, 2012.
- [2] J. Pan and W.-K. Ma, "Constant envelope precoding for single-user large-scale MISO channels: Efficient precoding and optimal designs," *IEEE J. Sel. Topics Signal Process.*, vol. 8, no. 5, pp. 982–995, 2014.
- [3] S. K. Mohammed and E. G. Larsson, "Per-antenna constant envelope precoding for large multi-user MIMO systems," *IEEE Trans. Commun.*, vol. 61, no. 3, pp. 1059–1071, 2013.
- [4] —, "Constant-envelope multi-user precoding for frequency-selective massive MIMO systems," *IEEE Wireless Commun. Lett.*, vol. 2, no. 5, pp. 547–550, 2013.
- [5] J.-C. Chen, C.-K. Wen, and K.-K. Wong, "Improved constant envelope multiuser precoding for massive MIMO systems," *IEEE Commun. Lett.*, vol. 18, no. 8, pp. 1311–1314, 2014.
- [6] P. V. Amadori and C. Masouros, "Constant envelope precoding by interference exploitation in phase shift keying-modulated multiuser transmission," *IEEE Trans. Wireless Commun.*, vol. 16, no. 1, pp. 538–550, 2017.
- [7] M. Shao, Q. Li, W.-K. Ma, and A. M.-C. So, "Minimum symbol error rate-based constant envelope precoding for multiuser massive MISO downlink," in *Proc. 2018 IEEE Statistical Signal Processing Workshop (SSP)*, June 2018, pp. 727–731.
- [8] M. Kazemi, H. Aghaeinia, and T. M. Duman, "Discrete-phase constant envelope precoding for massive MIMO systems," *IEEE Trans. Commun.*, vol. 65, no. 5, pp. 2011–2021, 2017.
- [9] H. Jedda, A. Mezghani, A. L. Swindlehurst, and J. A. Nossek, "Quantized constant envelope precoding with PSK and QAM signaling," *IEEE Trans. Wireless Commun.*, vol. 17, no. 12, pp. 8022–8034, Dec 2018.
- [10] S. Jacobsson, G. Durisi, M. Coldrey, T. Goldstein, and C. Studer, "Quantized precoding for massive MU-MIMO," *IEEE Trans. Commun.*, vol. 65, no. 11, pp. 4670–4684, 2017.
- [11] F. Sahrabi, Y.-F. Liu, and W. Yu, "One-bit precoding and constellation range design for massive MIMO with QAM signaling," *IEEE J. Sel. Topics Signal Process.*, vol. 12, no. 3, pp. 557–570, 2018.
- [12] M. Shao, Q. Li, and W.-K. Ma, "One-bit massive MIMO precoding via a minimum symbol-error probability design," in *Proc. 2018 IEEE International Conference on Acoustics, Speech and Signal Processing (ICASSP)*, April 2018, pp. 3579–3583.
- [13] M. Shao, Q. Li, W.-K. Ma, and A. M.-C. So, "A framework for one-bit and constant-envelope precoding over multiuser massive MISO channels," *arXiv preprint arXiv:1810.03159*, 2018.
- [14] A. Beck and M. Teboulle, "A fast iterative shrinkage-thresholding algorithm for linear inverse problems," *SIAM J. Imag. Sci.*, vol. 2, no. 1, pp. 183–202, 2009.
- [15] J. Tranter, N. D. Sidiropoulos, X. Fu, and A. Swami, "Fast unit-modulus least squares with applications in beamforming," *IEEE Trans. Signal Process.*, vol. 65, no. 11, pp. 2875–2887, 2017.